Article

Adsorption of Phosphate and Ammonium on Waste Building Sludge

Eva Bedrnová * , Barbora Doušová *, David Koloušek, Kateřina Maxová and Milan Angelis

Faculty of Chemical Technology, University of Chemistry and Technology Prague, Technická 5,
166 28 Prague 6, Czech Republic
* Correspondence: bedrnove@vscht.cz (E.B.); dousovab@vscht.cz (B.D.)

Abstract: Two selected waste building sludges (WBS) were used in this study: (i) sludge from the production and processing of prestressed concrete pillars (B) and (ii) sludge from the production of technical stone (TS). The materials were used in their original and Fe-modified forms (B_{Fe}/TS_{Fe}) for the adsorption of NH_4^+ and PO_4^{3-} from contaminated waters. The experiments were performed on a model solution simulating real wastewater with a concentration of 1.7 mmol·L^{-1} (NH_4^+) and 0.2 mmol·L^{-1} (PO_4^{3-}). The adsorption of PO_4^{3-} had a high efficiency (>99%) on B, B_{Fe} and TS_{Fe}, while for TS, the adsorption of PO_4^{3-} was futile due to the high content of available P in the raw TS. The adsorption of NH_4^+ on all sorbents (B/B_{Fe}, TS/TS_{Fe}) had a lower efficiency (<60%), while TS proved to be the most effective. Leaching tests were performed according to the CSN EN 12457 standard for B/B_{Fe} and TS/TS_{Fe} before and after NH_4^+ and PO_4^{3-} sorption when the contents of these ions in the leachates were affected by adsorption experiments in the cases of B and TS. For B_{Fe} and TS_{Fe}, the ion content in the leachates before and after the adsorption experiments was similar.

Keywords: adsorption; waste building sludge; Fe-modification

1. Introduction

In developed countries, the construction industry can create environmental issues, such as the depletion of natural resources and the production of several tons of construction waste [1,2]. Construction waste in various branches of the construction industry (the production of concrete, artificial stone, etc.) also includes dried powder building sludge (WBS), which is defined as a very fine material that is dispersed in water [1,2].

Concrete is one of the most widely used building materials, with an annual global consumption of 25 billion tons [3]. At present, various separation and recycling processes are used in its production, enabling the reuse of water and coarse aggregates [2,4,5]. The remaining concrete sludge (fine aggregates and cement particles) can be used in the production of ceramic materials [6], synthesis of geopolymers [7], or in the production of new concrete to reduce the required amount of cement [1,3,5].

All of these processes are relatively effective but insufficient for modern sustainable development. This is because the remaining concrete sludge (B) is landfilled without further use, along with several other wastes from the construction industry, such as powder waste from the production and treatment of technical stone (TS), which currently has no other application [4]. However, sewage sludges have a large specific surface area (S_{BET}), suitable structural properties and chemical composition (Si, Ca, Al and Fe content), which predetermine their possible applications in environmental technologies, for example, as adsorbents for removing toxic ions from contaminated waters [4,8,9].

Nitrogen and phosphorus in NH_4^+ and PO_4^{3-} ionic forms are an integral part of living organisms and plants [3,8,10]. Both elements are important for good plant growth and development and are often applied in the form of fertilizers to satisfy the growing requirement for food, but high concentrations of NH_4^+ and PO_4^{3-} in water result in excessive algae growth, which consumes dissolved oxygen and kill fishes and other organisms

living in the water (water eutrophication) [3,8,10–12]. High concentrations of NH_4^+ and PO_4^{3-} enter into natural streams from various sources, such as agricultural effluents, industrial wastewater and domestic wastewater [3,8,10–12]. Addressing the issue of declining reserves of mineable phosphate ore requires new solutions for capturing and reusing phosphates from wastewater [3,10–12]. Several types of absorbents (e.g., biochar, fly ashes, iron-enriched zeolites, etc.) have been developed for the regeneration of phosphates from wastewater [3,10–12]. The adsorption of NH_4^+ was studied, for example, on a polyurethane film prepared from ball-milled algal polyol particles to maintain low concentrations of this ion in fish and shrimp breeding tanks [13]. The coadsorption of NH_4^+ and PO_4^{3-} in wastewater was not discussed in these studies.

As part of this study, selective, simultaneous and additional adsorptions of NH_4^+ and PO_4^{3-} were monitored. The experimental data were fitted by the Langmuir and Freundlich adsorption isotherm to determine the sorption parameters ($q_{max.}$—maximum equilibrium adsorption capacity, Q_t—theoretical adsorption capacity, K_L—Langmuir adsorption constant, R^2—correlation factor, $1/n$—heterogeneity factor, K_F—Freundlich constant indicating adsorption capacity). The Langmuir adsorption isotherm is the simplified sorption model, which assumes the equivalence and even distribution of the active sites, to which only one series of non-interacting molecules can be bound [14–16]. The Freundlich adsorption isotherm is the first known model describing reversible multilayer adsorption with a different distribution of active sites [17]. Kinetic measurements were performed for NH_4^+ and PO_4^{3-} adsorption, and the data for systems that could be described by the Langmuir model (NH_4^+—TS, PO_4^{3-}— B, PO_4^{3-}—B_{Fe} and PO_4^{3-}—TS_{Fe}) were processed by pseudo-first- and pseudo-second-order formal kinetic models to find appropriate rate constants (k_1 for pseudo-first-order formal kinetic and k_2 for pseudo-second-order formal kinetic) [18].

The goal of this study was to find new possible applications of B and TS in their original and surface-modified forms (B_{Fe} and TS_{Fe}) for the coadsorption of NH_4^+ and PO_4^{3-} ions from wastewater and their subsequent use for improving the quality and nutritional values of agricultural soils.

2. Materials and Methods

2.1. Characterization of Used Building Waste Sludge

The WBS from the production of concrete (B) and artificial stone (TS) with a particle size of <0.1 mm was used. The B is formed during the production and abrasion of prestressed concrete columns, with a high cement content of ~21%. The TS is created during the production and processing of technical stone from Technistone, Czech Republic. The mineralogical and elemental composition of both materials were determined using X-ray powder diffraction (XRD) and X-ray fluorescence analysis (XRF), and the results are discussed further in Section 3.1.

For the selective sorption of anions, the surfaces of B and TS were modified with Fe^{2+} ions (B_{Fe}, TS_{Fe}) according to the verified method [19–22]. The surface modification was performed with 0.6 M $FeSO_4$ solution for 24 h at the laboratory temperature (20 °C) upon stirring the mixture with a shaker. Then, the suspension was filtered, and the obtained modified sludge was washed with distilled water, dried (60 °C) and homogenized.

2.2. Model Solution

The ion concentrations in the model solutions were chosen according to the real values in the wastewater (pond from the contaminated area) in the Havlíčkův Brod vicinity (Czech Republic—Highlands).

Model solutions of selected ions and their mixture were prepared in the concentration of 1.7 mmol·L^{-1} NH_4^+ and 0.2 mmol·L^{-1} PO_4^{3-}. The solutions were prepared from analytically pure inorganic salts NH_4Cl, K_2HPO_4 and distilled water at the original pH (~7.5).

Distilled water, tap water and 0.1 M KCl were used for leaching experiments.

2.3. Adsorption Experiments

The suspension of a defined amount of sorbent (5–40 g·L^{-1}) and 50 mL of model solution was shaken in 100 mL sealed polyethylene containers for 24 h (chosen based on preliminary experiments) at laboratory temperature (20 °C), pH of the model solution (~7.5) and at a speed of 280 rpm. Subsequently, vacuum filtration was performed on 0.6 μm pore size filters. The residual NH_4^+ and PO_4^{3-} concentrations in the obtained filtrates were analyzed.

The experimental data were fitted by the Langmuir and Freundlich adsorption isotherm to determine the sorption parameters ($q_{max.}$, Q_t, K_L, $1/n$, K_F, R^2). The accuracy of fitted data was supported by the triple measurement of the adsorption series.

The Langmuir isotherm is defined by Equation (1) [14–16]:

$$q = \frac{QKc}{1 + Kc},$$

(1)

and its linearized form by Equation (2) [14–16]:

$$\frac{1}{q} = \frac{1}{Q} + \frac{1}{QKc},$$

(2)

where q is an equilibrium concentration of an adsorbed ion in the solid phase [mmol·g^{-1}], c is an equilibrium concentration of an adsorbed ion in the solution [mmol·L^{-1}], Q_t is the theoretical adsorption capacity [mmol·g^{-1}], and K_L is a Langmuir adsorption constant [L mmol^{-1}].

The equilibrium ion concentration in the solid phase was calculated from the experimental data according to Equation (3) [14–16]:

$$q = \frac{V_0(c_0 - c)}{m},$$

(3)

where V_0 is the volume of solution [L], c_0 is the initial concentration of adsorbate in solution [mmol·L^{-1}], and m is the mass of the solid phase [g].

The Freundlich isotherm is defined by Equation (4) [17]:

$$q = K_F \cdot c^{1/n}$$

(4)

and its linearized form by Equation (5) [17]:

$$\log(q) = \log(K_F) + \frac{1}{n} \cdot \log(c)$$

(5)

where q is an equilibrium concentration of an adsorbed ion in the solid phase [mmol·g^{-1}], c is an equilibrium concentration of an adsorbed ion in the solution [mmol·L^{-1}], $1/n$ is the heterogeneity factor relating to adsorption intensity, and K_F is a Freundlich adsorption constant [mmol·g^{-1}]. The kinetic measurements were performed for NH_4^+ and PO_4^{3-} adsorption with 1.7 mmol·L^{-1} NH_4^+ and 0.2 mmol·L^{-1} PO_4^{3-} model solutions, the dosages of 10 g·L^{-1} (NH_4^+ adsorption) and 2.5 g·L^{-1} (PO_4^{3-} adsorption) and time intervals of 0.2, 1, 3, 5, 18.5, 24, 28 and 48 h.

Kinetic data for the systems that could be described by the Langmuir model (NH_4^+—TS, PO_4^{3-}—B, PO_4^{3-}—B_{Fe} and PO_4^{3-}—TS_{Fe}) were processed by the pseudo-first- and the pseudo-second-order formal kinetic models to find rate constants (k_1 and k_2) [18].

The pseudo-first-order kinetic model is described by Equation (6) [18]:

$$\frac{dq_t}{dt} = k_1(q_e - q_t)$$

(6)

Integrated Equation (4) and substituted the boundary conditions from t = 0 to t = t and $q_t = 0$ to $q_t = q_t$, a linearized equation was obtained (Equation (7) [18]:

$$\ln(q_e - q_t) = \ln(q_e) - k_1 t$$

(7)

The pseudo-second-order kinetic model is described by Equation (8) [18]:

$$\frac{dq_t}{dt} = k_2(q_e - q_t)^2 \tag{8}$$

Integrated Equation (6) and substituted the boundary conditions from t = 0 to t = t and $q_t = 0$ to $q_t = q_t$, a linearized equation was obtained (Equation (9) [18]:

$$\frac{t}{q_t} = \frac{1}{h} + \frac{1}{q_e}t \tag{9}$$

$$h = k_2 q_e^2$$

where t is time [h], q_t is a concentration of an adsorbed ion in the solid phase at time t [mmol·g^{-1}], qe is an equilibrium concentration of an adsorbed ion in the solid phase [mmol·g^{-1}], k_1 is pseudo-first-order formal kinetic rate constant [h^{-1}] and k_2 is a pseudo-second-order formal kinetic rate constant [g·mmol^{-1}·h^{-1}].

2.4. Leaching Tests

The leaching of both ions from the original and saturated WBS was performed according to the CSN EN 12,457 standard [23]. The defined amounts of B and TS before and after the sorption of NH_4^+ and PO_4^{3-} were poured with the appropriate leaching solution (Section 2.2) at the solid–liquid ratio of 1:10.

2.5. Analytical Methods

X-ray powder diffraction (XRD) of solid samples was measured using a 2D Phaser (Bruker s.r.o., Billerica, MA, USA). A current of 10 mA, a voltage of 30 kV, a step size of 0.02° and a range of angles (6–80 2θ) were used for the measurements.

The semi-quantitative chemical composition was determined by X-ray fluorescence analysis (XRF), which was performed using a NEX QC instrument (Rigaku Company, Tokio, Japan), where the powder sludge was measured at 50 kV using an SDD detector.

Zero-charge pH (pH$_{zpc}$) was measured using the Stabino®, Version 2.0 (Particle Metrix GmbH, Inning am Ammersee, Germany). The stabilized suspensions of the solid sample and 0.1, 0.01 and 0.001 M KCl (solid: liquid ratio of 1:100) were dynamic with 0.1 M solution of NaOH or HCl to the isoelectric point (IEP). The resulting pHzpc value is the average of three pH values corresponding to the zero potential.

The Micromeritics ASAP 2020 (accelerated surface area and porosimetry) analyzer (Micromeritics®, Norcross, GA, USA) was used to measure the specific surface area (S$_{BET}$) of the sludge used, which uses gas sorption (N_2) to study macropores and micropores using the Horvath–Kavazoe method (BJH method) bath at −195.8 °C. Prior to measurement, the samples were degassed at 313 K for 1000 min.

NH_4^+ and PO_4^{3-} concentrations were determined by UV/Vis spectrophotometry using an Evolution 220 instrument (Thermo Scientific®, Waltham, MA, USA) at 425 nm for NH_4^+ using potassium sodium tartrate and Nessler reagent [24], and at 820 nm for PO_4^{3-} using the molybdenum blue method [25].

3. Results and Discussion

3.1. Characterization of Original and Modified B/BFe and TS/TSFe

From the XRD diffractograms (Figure 1) of the original waste building sludge, B (Figure 1a) is characterized by portlandite and calcite. The aggregate used in the concrete was granite; the filler used in TS (Figure 1b) was quartz.

The XRD diffractograms for B$_{Fe}$ and TS$_{Fe}$ were identical to their original forms of B and TS (Figure 1) because Fe oxides were bound to the silicate skeleton of B or TS by chemisorption in an amorphous form during the modification of Fe^{2+} ions when hydrated metal particles formed on the surface of the sorbents (B$_{Fe}$, TS$_{Fe}$) in reactive, ion-exchangeable positions and there were no changes in mineralogical composition [17,18]. The chemical and surface

properties were changed by the modification with Fe^{2+} ions; the B_{Fe} and TS_{Fe} significantly differed in S_{BET}, Fe and alkali content (Table 1), which affected PO_4^{3-} and NH_4^+ adsorption. The chemical and surface properties of B, TS, B_{Fe} and TS_{Fe} are listed in Table 1.
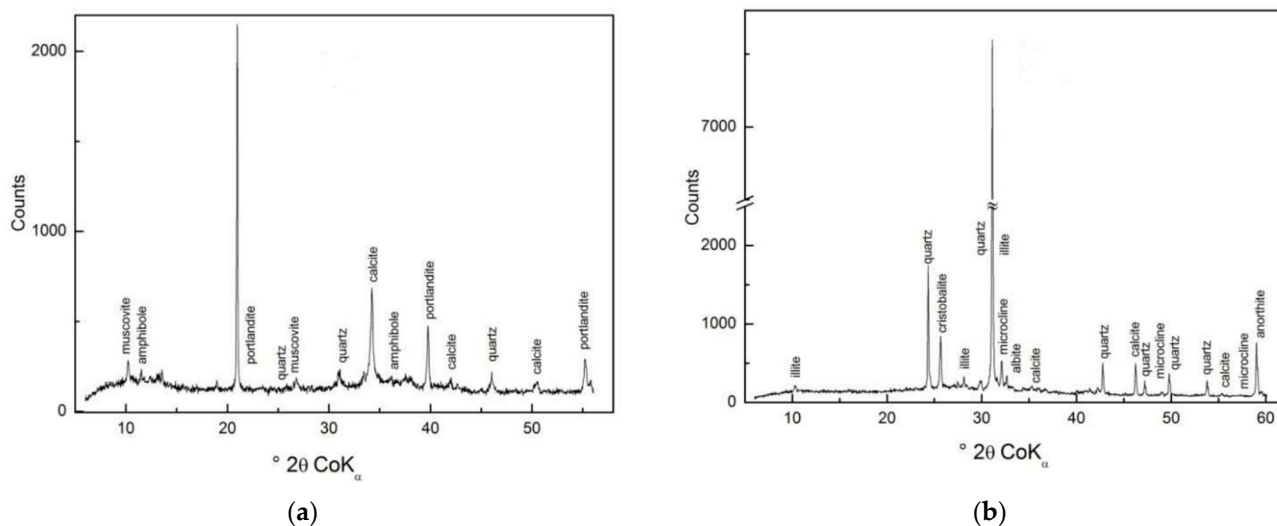
Figure 1. XRD patterns of WBS: (**a**) B; (**b**) TS.

Table 1. Chemical and surface properties of B/B_{Fe} and TS/TS_{Fe}.

Sample	Chemical Composition (% wt.)							S_{BET} $(m^2 \cdot g^{-1})$	pH_{ZPC}
	SiO_2	Al_2O_3	Fe_2O_3	TiO_2	CaO	MgO	P_2O_5		
B	32.3	6.6	1.3	<0.1	46.9	1.8	0.2	38.2	10.3
B_{Fe}	26.6	4.3	29.8	0.4	18.7	2.1	0.1	118.2	7.5
TS	85.3	35.0	0.01	0.0	3.6	1.8	0.6	2.1	6.2
TS_{Fe}	75.6	28.9	5.4	0.06	2.8	1.9	0.4	14.9	6.7

3.2. Adsorption of the Selected Ion (NH_4^+ or PO_4^{3-}) on Original and Modified B/B_{Fe} and TS/TS_{Fe}

All adsorption experiments were performed under the same conditions described in Section 2.3. Figure 2 shows the dependence of adsorption efficiencies ε (%) on the weight m ($g \cdot L^{-1}$) of B/B_{Fe} and TS/TS_{Fe} for NH_4^+ or PO_4^{3-}. Table 2 shows the sorption parameters (theoretical adsorption capacities—Q_t; adsorption constants—K_L and K_F; heterogeneity factor—$1/n$; root mean squared error—RMSE) calculated using the Langmuir and Freundlich model [14–16].

PO_4^{3-} adsorption occurred with high efficiency (<99%) on modified forms B_{Fe} and TS_{Fe} (Figure 2b). Due to its high alkalinity, B did not primarily support the adsorption of anions. The high efficiency of PO_4^{3-} adsorption on B can be explained by the precipitation of PO_4^{3-} into a poorly soluble amorphous form or as apatite ($Ca_5(PO_4)_3$ (OH)). Modified forms of B_{Fe} (Figure 2b, orange line) and TS_{Fe} (Figure 2b, red line) achieved high sorption efficiencies with PO_4^{3-} because they were enriched with hydrated metal particles in reactive, ion-exchangeable surface positions (Section 3.1). These available Fe ions are sufficient for the adsorption of an oxyanion such as PO_4^{3-} onto Fe oxy(hydroxides). The TS released PO_4^{3-} into the solution, where the concentration of this ion increased by more than 50% at the highest dosage of sorbent (Figure 2b, blue line).

NH_4^+ adsorption occurred with lower efficiency (<60%), whereas the TS proved to be most effective (Figure 2a, blue line). The sorption efficiency of NH_4^+ adsorption on B decreased with the increase in sorbent dosage (Figure 2a, green line) due to the alkaline nature of B. The pH of the solution increased more rapidly when the dosage of B increased, and the solution became alkaline (~12) very quickly at the highest dose of B. The NH_4^+ ion in an alkaline environment is converted to NH_3 and cannot be absorbed onto the surface of the sorbent.

(**a**)

(**b**)
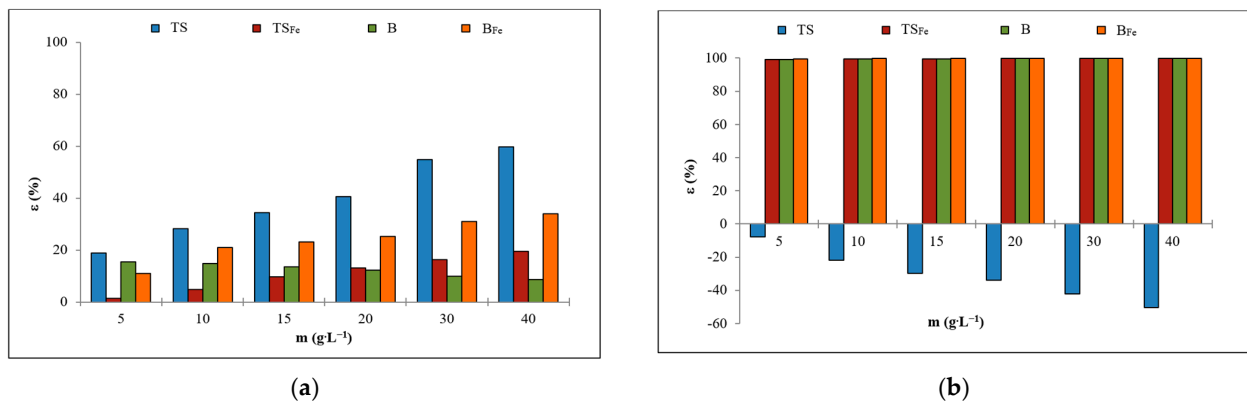
Figure 2. Adsorption efficiencies of B/B_{Fe} and TS/TS_{Fe} for selected ions: (**a**) NH_4^+; (**b**) PO_4^{3-}.

Table 2. Adsorption parameters for NH_4^+ and PO_4^{3-} on B, TS, B_{Fe} and TS_{Fe}.

Ion	Sorbent	$q_{max.}$ (mmol·g^{-1})	Langmuir Model				Freundlich Model			
			Q_t * (mmol·g^{-1})	K_L * (L·mmol^{-1})	R^2 *	RMSE	1/n *	K_F * (mmol·g^{-1})	R^2 *	RMSE
NH_4^+	B	0.06	-**	-**	-**	-**	-**	-**	-**	-**
	B_{Fe}	0.04	-**	-**	-**	-**	0.95	0.008	0.565	0.001
	TS	0.06	0.09	0.62	0.897	0.004	0.62	0.032	0.894	0.002
	TS_{Fe}	0.01	-**	-**	-**	-**	0.96	0.005	0.496	0.001
PO_4^{3-}	B	0.06	0.03	1922.39	0.944	0.011	0.69	2.36	0.935	0.006
	B_{Fe}	0.07	0.07	1868.00	0.966	0.007	0.80	8.89	0.952	0.004
	TS	-***	-**	-**	-**	-**	-**	-**	-**	-**
	TS_{Fe}	0.06	0.04	1439.24	0.978	0.007	0.68	2.33	0.956	0.004

* Calculated adsorption parameters based on the adsorption model (Section 2.3.); ** did not follow adsorption model; *** PO_4^{3-} was released into the solution instead of sorption.

The adsorption of PO_4^{3-} on B, B_{Fe} and TS_{Fe} and NH_4^+ on TS corresponded to both the Freundlich and Langmuir models, but the worse correlation of experimental data for the Freundlich model (R^2: 0.496–0.956 versus 0.897–0.999, Table 2) indicated the Langmuir isotherm more appropriate for investigated systems. The NH_4^+ adsorption on B_{Fe} a TS_{Fe} followed the Freundlich model but with very low correlation factors.

Kinetic experiments were performed under the same conditions described in Section 2.3. The dependence of concentration q_t (mmol·g^{-1}) of an adsorbed ion (NH_4^+ or PO_4^{3-}) in the solid phase on the contact time t (h) is shown in Figure 3.

(**a**)

(**b**)
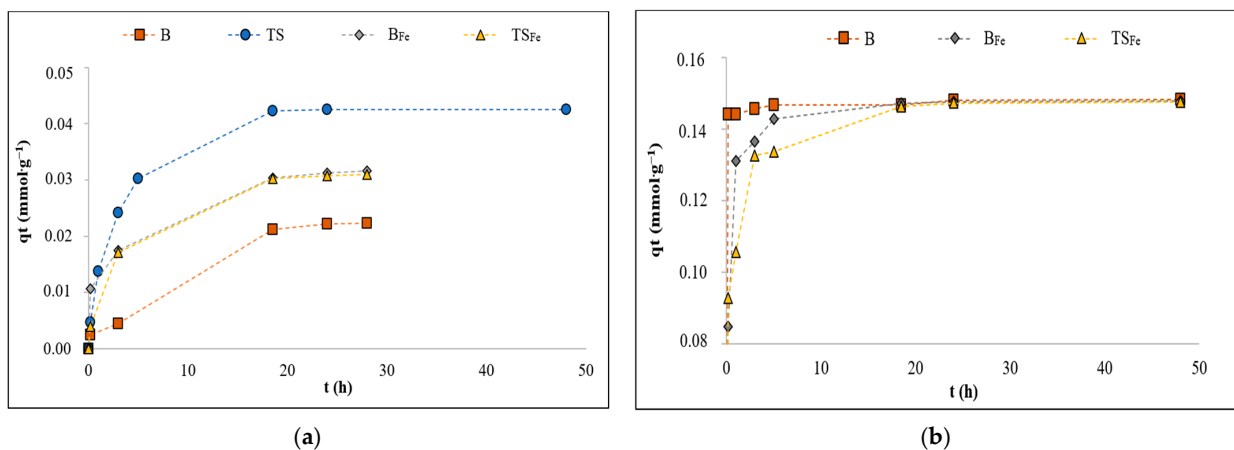
Figure 3. Adsorption kinetics of B/B_{Fe} and TS/TS_{Fe} for selected ions: (**a**) NH_4^+; (**b**) PO_4^{3-}.

The PO_4^{3-} and NH_4^+ adsorption equilibrium was reached around 19 h (Figure 3).

The obtained rate constants (k_1 and k_2) and correlation factors (R^2) for the pseudo-first- and the pseudo-second-order formal kinetic models, which were used for the systems that could be fitted by the Langmuir model (Section 2.3), are reported in Table 3.

Table 3. Correlation factors (R^2) and velocity constants (k_1 and k_2) of the pseudo-first-order kinetics model and the pseudo-second-order kinetics model.

Adsorption System	Pseudo-First-Order Kinetics Model		Pseudo-Second-Order Kinetics Model	
	R^2	k_1 (h^{-1})	R^2	k_2 (g·mmol^{-1}·h^{-1})
PO_4^{3-}—B	0.782	0.11	0.999	124.8
PO_4^{3-}—B$_{Fe}$	0.934	0.20	0.999	39.3
PO_4^{3-}—TS$_{Fe}$	0.983	0.21	0.999	20.3
NH_4^+—TS	0.983	0.31	0.999	11.6

Adsorption systems that could be fitted to the Langmuir model (PO_4^{3-}—B, PO_4^{3-}—B$_{Fe}$, PO_4^{3-}—TS$_{Fe}$ and NH_4^+—TS) proceeded by chemisorption, according to the pseudo-second-order kinetic model (Section 2.3). The other studied systems did not correlate sufficiently with any of the applied adsorption models, and prevailing physical adsorption could be assumed.

3.3. Additional Adsorption of NH_4^+ and PO_4^{3-} on Original and Modified B/B$_{Fe}$ and TS/TS$_{Fe}$

In order to determine the possible accumulation of NH_4^+ or PO_4^{3-} and the effect of adsorbed NH_4^+ or PO_4^{3-} on the possibility of further sorption, the most effective systems of selected adsorption (Section 3.2) were saturated with the oppositely charged ion. Figure 4 compares the sorption efficiencies of the ions adsorbed in the selective sorption (Sec.) and in the additional sorption (Add.) on the oppositely charged ion captured on the sorbent surface during the prior selective sorption (Section 3.2). Additionally, the PO_4^{3-}—B, PO_4^{3-}—B$_{Fe}$ and PO_4^{3-}—TS$_{Fe}$ systems were used for NH_4^+ adsorption, while for the PO_4^{3-} adsorption, only the NH_4^+—TS system was used.
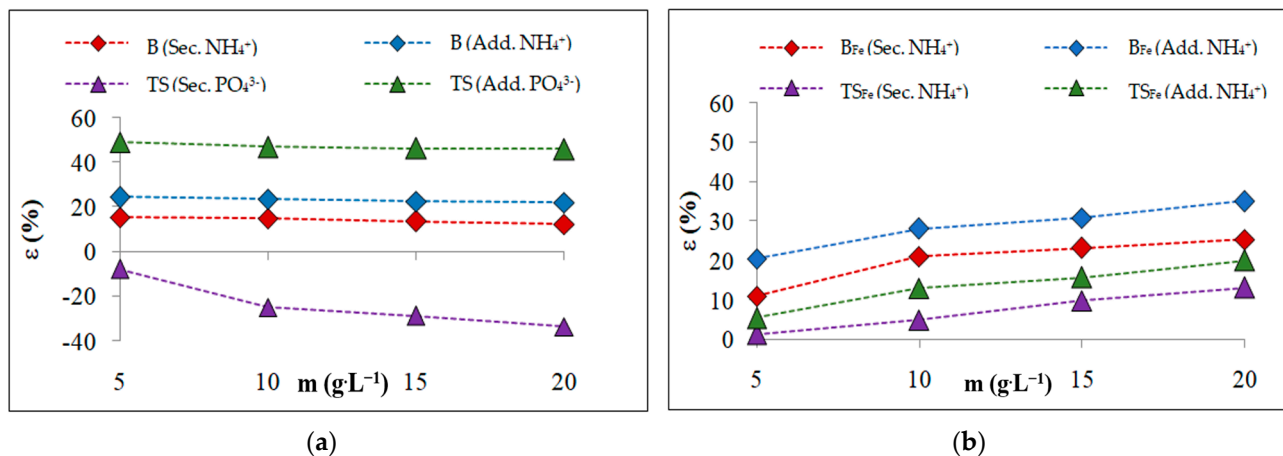
Figure 4. Changes in sorption efficiency for selective and additional sorptions: (**a**) B, TS; (**b**) B$_{Fe}$, TS$_{Fe}$.

During the additional adsorption, the sorption efficiency increased from 6% for adsorption NH_4^+ on PO_4^{3-}—TS$_{Fe}$ system (Figure 4b) to 60% for adsorption of PO_4^{3-} on the NH_4^+—TS system (Figure 4a) because active sites formed on the surfaces of the formerly saturated sorbents with NH_4^+ or PO_4^{3-}, causing the additional binding of oppositely charged ions, whereby the adsorption yield of additional adsorption increased. These active sites also supported the accumulation of nutrients in the sorbents for possible applications in agricultural soils.

3.4. Simultaneous Adsorption of NH_4^+ and PO_4^{3-} on Original and Modified B/B_{Fe} and TS/TS_{Fe}

The tested ions can usually coexist in real water systems; therefore, their simultaneous sorptions (Sim.) on B, TS, B_{Fe} and TS_{Fe} were performed. Figure 5 shows the dependence of the adsorption efficiencies on the dosage of B/B_{Fe} and TS/TS_{Fe} for NH_4^+ (Figure 5a) and PO_4^{3-} (Figure 5b) adsorption when the data obtained in this sorption experiment are compared with the sorption efficiencies of selective ion sorption (Sec.) mentioned in Section 3.2.

(a)

(b)
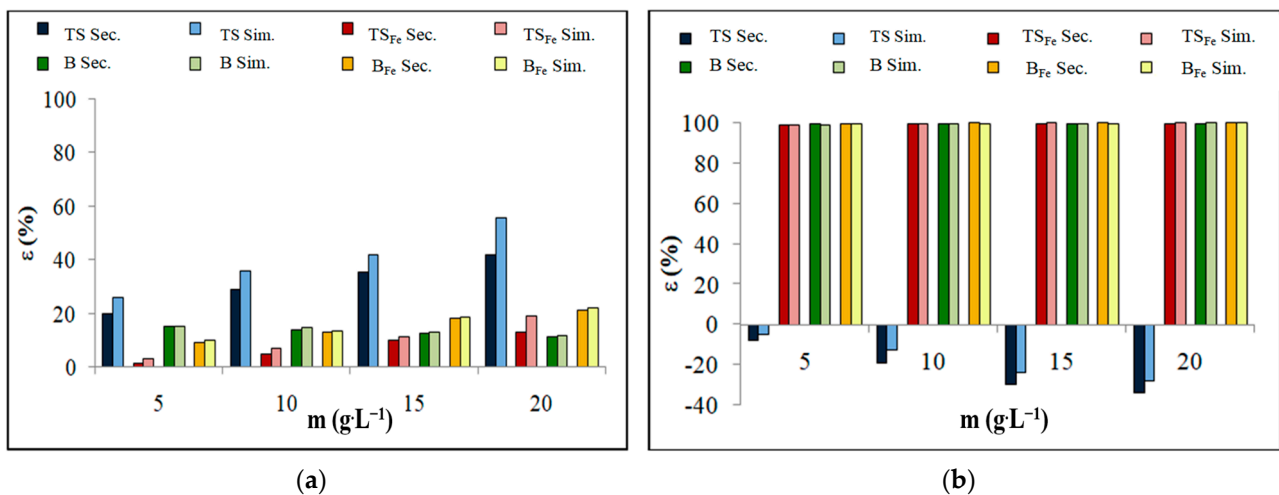
Figure 5. Adsorption efficiencies of B/B_{Fe} and TS/TS_{Fe} for selected ion sorption and simultaneous sorption: (**a**) NH_4^+; (**b**) PO_4^{3-}.

The simultaneous sorption of PO_4^{3-} on B, B_{Fe} and TS_{Fe} (Figure 5b) was very efficient (>99% adsorption efficiency) in the presence of NH_4^+ in the solution. The efficiency of the simultaneous sorption for PO_4^{3-} is very similar to the efficiency of the selective adsorption of the PO_4^{3-} ion. The simultaneous sorption of PO_4^{3-} on TS remained ineffective (light and dark blue lines in Figure 5b).

The efficiency of adsorption of NH_4^+ in the simultaneous presence of PO_4^{3-} in the solution was higher for all sorbents when compared to the adsorption efficiency of the selective adsorption of the NH_4^+ ion (Figure 5a); it is possible that a similar situation occurred, as in the case of additional sorption experiments (Section 3.3).

3.5. Leaching Experiments

The leaching experiments (described in Section 2.4) were performed to determine the possible use of both sludges (B and TS) as additives to agricultural soils to improve their quality. Figures 5 and 6 show the amounts of NH_4^+/PO_4^{3-} ions leached from the individual sludges (B/B_{Fe} and TS/TS_{Fe}) before (Figure 6) and after (Figure 7) the adsorption of selected ions.

The leaching experiments revealed a relatively high release of PO_4^{3-} (Figures 6b and 7b) and NH_4^+ (Figures 6a and 7a) from saturated and original sorbents, B and TS. For the B and TS, the leaching tests also showed that the leaching of PO_4^{3-} and NH_4^+ was affected by the saturation of the PO_4^{3-} or NH_4^+ on the sorbent surface (PO_4^{3-} and NH_4^+ adsorption is discussed in Sections 3.2–3.4).

The B_{Fe} and TS_{Fe} were able to leach significantly lower contents than their original forms B and TS, and due to their affinity for oxyanions, PO_4^{3-} was almost not leached (Figures 6b and 7b, yellow and grey lines).

The content of NH_4^+ in the leachates decreased in the following order: $TS_{sorption} > B > B_{Fe\ sorption} \cong B_{Fe} > B_{sorption} > TS > TS_{Fe\ sorption} \cong TS_{Fe}$. The content of PO_4^{3-} in the leachates decreased in the following order: $TS >> TS_{sorption} > B_{sorption} > B > TS_{Fe\ sorption} \cong TS_{Fe} > B_{Fe\ sorption} \cong B_{Fe}$.
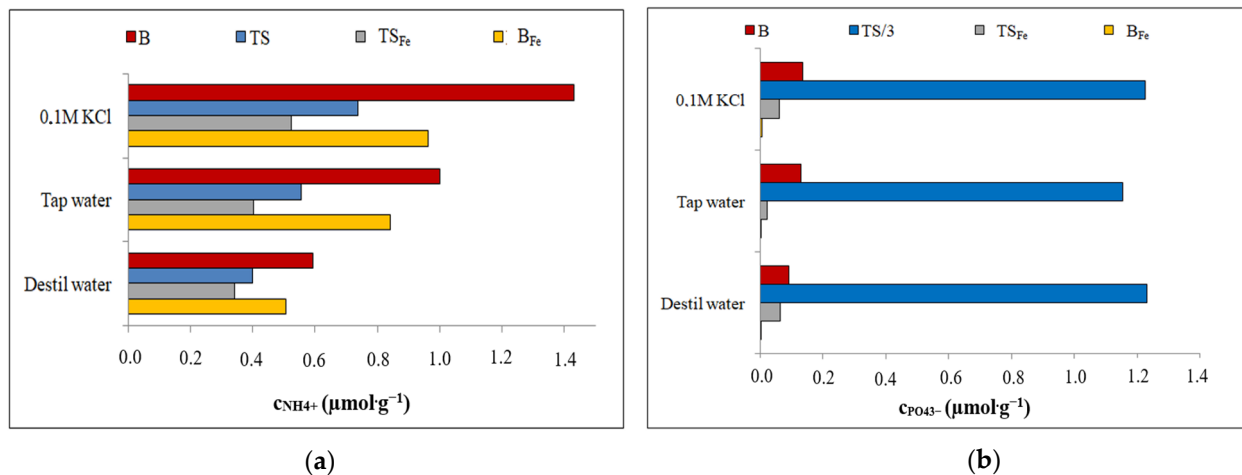
Figure 6. The amount of ion leached from B/B$_{Fe}$ and TS/TS$_{Fe}$ before adsorption: (**a**) NH$_4^+$; (**b**) PO$_4^{3-}$.
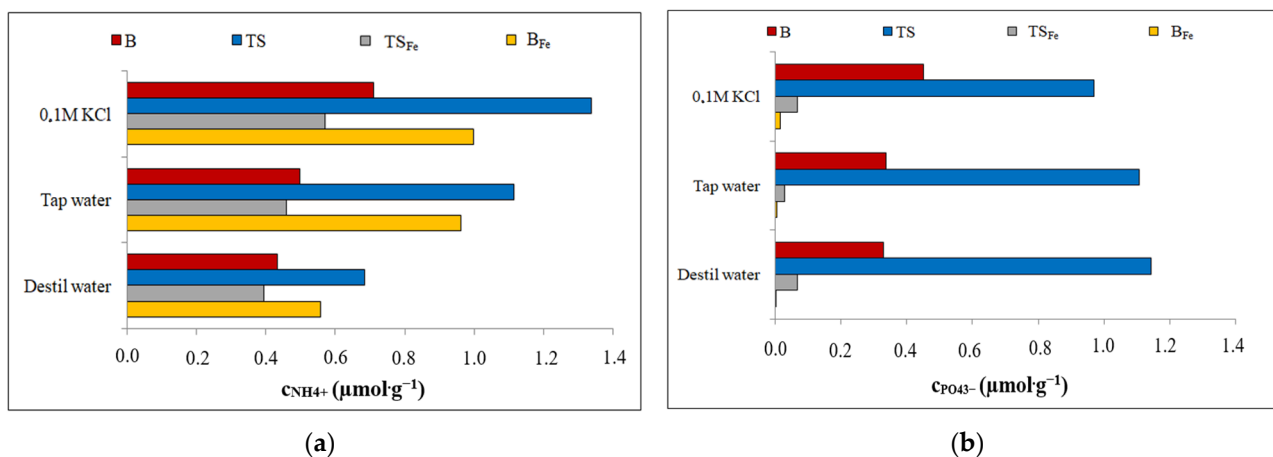
Figure 7. The amount of ion leached from B/B$_{Fe}$ and TS/TS$_{Fe}$ after selected ion adsorption: (**a**) NH$_4^+$; (**b**) PO$_4^{3-}$.

4. Conclusions

B, B$_{Fe}$ and TS$_{Fe}$ proved to be promising sorbents for the sorption of PO$_4^{3-}$ when such adsorptions were successfully fitted by the Freundlich and Langmuir adsorption models, with better parameters for the Langmuir fit. The TS spontaneously released PO$_4^{3-}$ into the solution, and no adsorption occurred.

The adsorption of NH$_4^+$ had a lower efficiency compared to the sorption of PO$_4^{3-}$, while the TS was found to be the most efficient sorbent. The adsorption of NH$_4^+$ on the TS could be fitted by the Freundlich and Langmuir adsorption models when better correlation factors were achieved for the Langmuir fit. The NH$_4^+$ adsorption on B$_{Fe}$ and TS$_{Fe}$ followed the Freundlich model but with very low correlation factors. Adsorption of NH$_4^+$ proceeded with a lower sorption robustness compared to the PO$_4^{3-}$ adsorption.

The kinetic equilibrium for PO$_4^{3-}$ and NH$_4^+$ adsorption was reached around 19 h. For the selected adsorption systems that could be fitted by the Langmuir model (PO$_4^{3-}$ adsorption on B, B$_{Fe}$ and TS$_{Fe}$ and NH$_4^+$ adsorption on TS), the pseudo-second-order kinetic model was the most suitable, and these adsorption systems proceeded by chemisorption.

During the adsorption of oppositely charged ions on the sorbents formerly saturated with NH$_4^+$ or PO$_4^{3-}$ (i.e., the NH$_4^+$ adsorption on B, B$_{Fe}$ and TS$_{Fe}$ saturated with PO$_4^{3-}$, and the PO$_4^{3-}$ adsorption on TS saturated with NH$_4^+$) the efficiency increased compared to the adsorption on the original sorbents due to the creation of new active sites on the sorbent surface. The simultaneous sorption of PO$_4^{3-}$ and NH$_4^+$ was more efficient when compared with the efficiency of selective ion adsorption.

The leaching experiments proved to have a relatively high release of PO_4^{3-} and NH_4^+ from saturated sorbents, which made it possible to apply the saturated sorbents to agricultural soils, for example, to increase their nutritional values. The content of NH_4^+ in the leachates decreased in the following order: $TS_{sorption}$ > B > $B_{Fe\ sorption}$ ≅ B_{Fe} > $B_{sorption}$ > TS > $TS_{Fe\ sorption}$ ≅ TS_{Fe}; the content of PO_4^{3-} in the leachates decreased in the following order: TS > $TS_{sorption}$ > $B_{sorption}$ > B > $TS_{Fe\ sorption}$ ≅ TS_{Fe} > $B_{Fe\ sorption}$ ≅ B_{Fe}.

The waste concrete sludge B was found to be an effective PO_4^{3-} sorbent. It is unsuitable for NH_4^+ sorption due to its high alkalinity, which can be considered a major disadvantage for its possible use as a soil additive. Waste from the production of artificial stone TS was found to be a relatively good sorbent for the NH_4^+, but a high dosage is necessary to achieve an acceptable sorption efficiency. For the sorption of PO_4^{3-}, the TS is completely unsuitable because of the spontaneous release of this ion into the solution. Due to significantly lower alkalinity, the TS represents a promising candidate for application to agricultural soils. The modified B_{Fe} and TS_{Fe} forms proved to be selective and efficient sorbents of PO_4^{3-} ions, while the adsorption of NH_4^+ on B_{Fe} and TS_{Fe} was almost ineffective. The use of B_{Fe} and TS_{Fe} as soil additives was possible.

References

1. Correia, S.; Souza, F.; Dienstmann, G.; Segadães, A. Assessment of the recycling potential of fresh concrete waste using a factorial design of experiments. *Waste Manag.* **2009**, *29*, 2886–2891. [CrossRef] [PubMed]
2. Xuan, D.; Zhan, B.; Poon, C.S.; Zheng, W. Innovative reuse of concrete slurry waste from ready-mixed concrete plants in construction products. *J. Hazard. Mater.* **2016**, *312*, 65–72. [CrossRef] [PubMed]
3. dos Reis, G.S.; Thue, P.S.; Cazacliu, B.G.; Lima, E.C.; Sampaio, C.H.; Quattrone, M.; Ovsyannikova, E.; Kruse, A.; Dotto, G.L. Effect of concrete carbonation on phosphate removal through adsorption process and its potential application as fertilizer. *J. Clean. Prod.* **2020**, *256*, 120416. [CrossRef]
4. Doušová, B.; Bedrnová, E.; Reiterman, P.; Keppert, M.; Koloušek, D.; Lhotka, M.; Mastný, L. Adsorption Properties of Waste Building Sludge for Environmental Protection. *Minerals* **2021**, *11*, 309.
5. Martins, V.J.; Garcia, S.C.D.; Aguilar, P.T.M.; José dos Santos, W. Influence of replacing Portland cement with three different concrete sludge wastes. *Constr. Build. Mater.* **2021**, *303*, 124519. [CrossRef]
6. Schoon, J.; De Buysser, K.; Van Driessche, I.; De Belie, N. Feasibility Study of the Use of Concrete Sludge As Alternative Raw Material for Portland Clinker Production. *J. Mater. Civ. Eng.* **2015**, *27*, 04014272. [CrossRef]
7. Yang, Z.X.; Ha, N.R.; Hwang, K.H.; Lee, J.K. A Study of the performance of a concrete sludge-based geopolymer. *J. Ceram. Process. Res.* **2009**, *10*, S72–S74.
8. Dos Reis, S.G.; Cazacliu, G.B.; Correa, R.C.; Ovsyannikova, E.; Andrea Kruse, A.; Sampaio, H.C.; Lima, C.E.; Dotto, L.G. Adsorption and recovery of phosphate from aqueous solution by the construction and demolition wastes sludge and its potential use as phosphate-based fertilizer. *J. Environ. Chem. Eng.* **2020**, *8*, 103605.

9. Doušová, B.; Reiterman, P.; Keppert, M.; Lhotka, M.; Koloušek, D.; Mastný, L.; Bedrnová, E. Assumptions of Powdered Building Wastes for Selective Adsorption of Lead and Cesium from Water. *AIP Conf. Proc.* **2020**, *2210*, 020006.

10. Sun, D.; Hale, L.; Kar, G.; Soolanayakanahally, R.; Adl, S. Phosphorus recovery and reuse by pyrolysis: Applications for agriculture and environment. *Chemosphere* **2018**, *194*, 682–691. [CrossRef]

11. Guaya, D.; Cobos, H.; Camacho, J.; López, C.M.; Valderrama, C.; Cortina, J.L. LTA and FAU-X Iron-Enriched Zeolites: Use for Phosphate Removal from Aqueous Medium. *Materials* **2022**, *15*, 5418. [CrossRef] [PubMed]

12. Hermassi, M.; Valderrama, C.; Moreno, N.; Font, O.; Querol, X.; Batis, N.H.; Cortina, J.L. Fly ash as reactive sorbent for phosphate removal from treated waste water as a potential slow release fertilizer. *J. Environ. Chem. Eng.* **2016**, *5*, 160–169. [CrossRef]

13. Iqhrammullah, M.; Saleha, S.; Maulina, F.P.; Idroes, R. Polyurethane film prepared from ball-milled algal polyol particle and activated carbon filler for NH_3–N removal. *Heliyon* **2020**, *6*, e04590. [CrossRef]

14. Doušová, B.; Koloušek, D.; Lhotka, M.; Keppert, M.; Urbanová, M.; Kobera, L.; Brus, J. Waste Brick Dust as Potential Sorbent of Lead and Cesium from Contaminated Water. *Materials* **2019**, *12*, 1647. [CrossRef] [PubMed]

15. Doušová, B.; Koloušek, D.; Keppert, M.; Machovic, V.; Lhotka, M.; Urbanova, M.; Holcova, L. Use of waste ceramics in ad-sorption technologies. *Appl. Clay Sci.* **2016**, *8*, 145–152. [CrossRef]

16. Jeong, Y.; Fan, M.; Singh, S.; Chuang, C.-L.; Saha, B.; van Leeuwen, J.H. Evaluation of iron oxide and aluminum oxide as potential arsenic(V) adsorbents. *Chem. Eng. Process.-Process Intensif.* **2007**, *46*, 1030–1039. [CrossRef]

17. Wang, C.; Boithias, L.; Ning, Z.; Han, Y.; Sauvage, S.; Sánchez-Pérez, J.-M.; Kuramochi, K.; Hatano, R. Comparison of Langmuir and Freundlich adsorption equations within the SWAT-K model for assessing potassium environmental losses at basin scale. *Agric. Water Manag.* **2017**, *180*, 205–211. [CrossRef]

18. Maji, S.K.; Pal, A.; Pal, T. Arsenic removal from real-life groundwater by adsorption on laterite soil. *J. Hazard. Mater.* **2008**, *151*, 811–820. [CrossRef]

19. Doušová, B.; Grygar, T.; Martaus, A.; Fuitová, L.; Koloušek, D.; Machovič, V. Sorption of AsV on aluminosilicates treated with FeII nanoparticles. *J. Colloid Interface Sci.* **2006**, *302*, 424–431.

20. Bonnin, D. Method of removing arsenic species from an aqueous medium using modified zeolite minerals. U.S. Patent No. 6,042,731, 28 March 2000.

21. Doušová, B.; Fuitová, L.; Grygar, T.; Machovič, V.; Koloušek, D.; Herzogová, L.; Miloslav, L. Modified aluminosilicates as low-cost sorbents of As(III) from anoxic groundwater. *J. Hazard. Mater.* **2009**, *165*, 134–140.

22. Doušová, B.; Machovič, V.; Lhotka, M.; Reiterman, P.; Bedrnová, E.; Koloušek, D. Mechanism of chromate adsorption on Fe-modified concrete slurry waste. *Colloids Surf. A* **2022**, *650*, 129650. [CrossRef]

23. CEN. *Characterization of Waste-Leaching-Compliance Test for Leaching of Granular Waste Materials and Sludges. Part 2. One Stage Batch Test at a Liquid to Solid Ratio of 10 L/kg for Materials with Particle Size below 4 mm (without or with Size Reduction), EN 12457-2*; Comite Europeen de Normalisation: Brussels, Belgium, 2002.

24. Stanovení Amoniakálního Dusíku ve Vodě, 2007. Masarykova Střední Škola Chemická: Návody na Chemické Rozbory. Available online: http://old.mssch.cz/2004-2009/old.mssch.cz/index9b0f.html?kat=189&idclanek=692 (accessed on 2 February 2022).

25. Malát, M. Metody stanovení fosforu. In *Absorpční Anorganická Fotometrie*; Academia: Prague, Czech Republic, 1973; pp. 470–473.